

1 **Supplementary Material 1: Anisotropic Viscosity Scheme**

2 Horizontal viscosity is required in ocean circulation models to resolve the western boundary
3 currents and to smooth out numerical noise [*Munk*, 1950; *Bryan et al.*, 1975; *Large et al.*, 2001].
4 Isotropic viscosity schemes apply one large viscosity value needed for these purposes
5 everywhere in the model which is not physically realistic outside of these specific areas. A
6 major deficiency when using isotropic viscosities is the underestimation of the Pacific Equatorial
7 Undercurrent which in models is typically about 10% compared to what is observed [*Large et*
8 *al.*, 2001]. The Pacific Equatorial Undercurrent is a source of relatively warm, fresh, nutrient-
9 poor and oxygen-rich water from the Western Pacific that flows into the Eastern Pacific which
10 has important physical and biogeochemical effects. We implement an anisotropic viscosity
11 scheme similar to *Large et al.* [2001] in the tropics to better resolve equatorial dynamics. Figure
12 S1-1 shows zonal and meridional surface viscosities used and Figure S1-2 shows a comparison at
13 125°W of the simulated currents with observations in the Eastern Tropical Pacific [*Kessler*,
14 2006], the region most significantly affected by the anisotropic viscosity scheme.

15

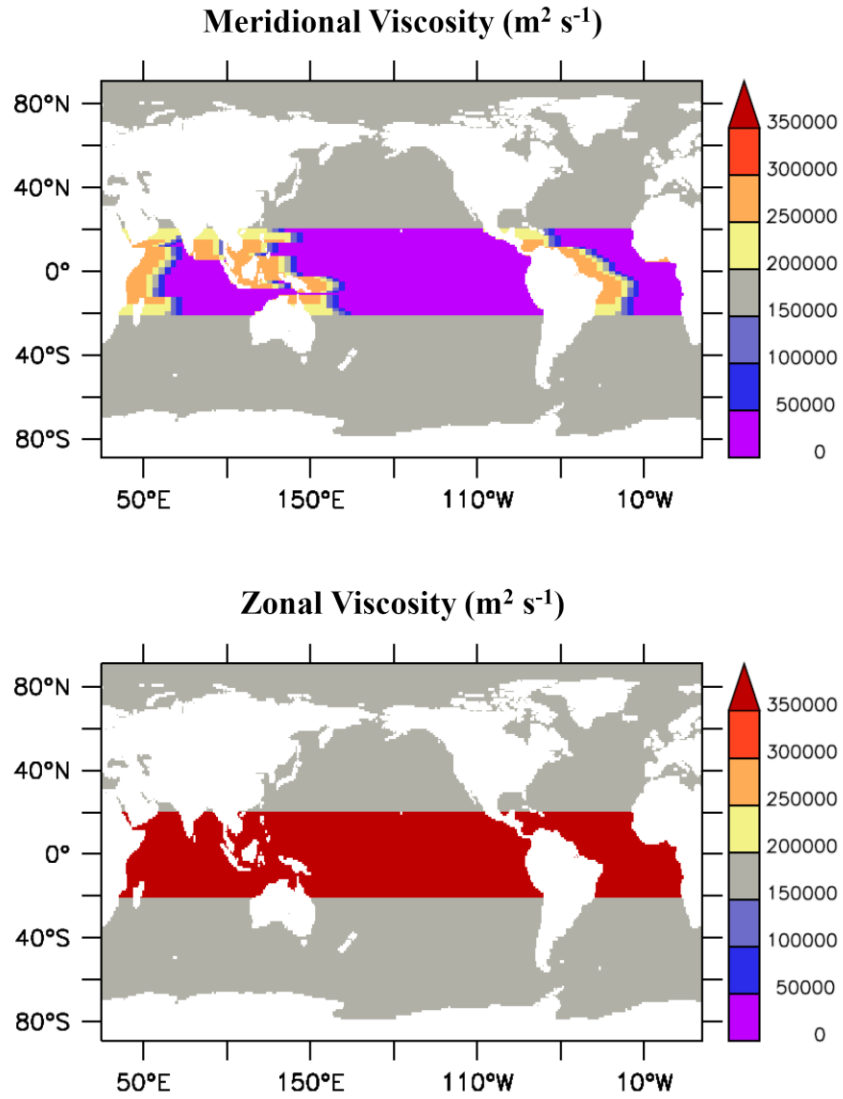


Figure S1-1. Surface viscosity in the meridional and zonal directions.

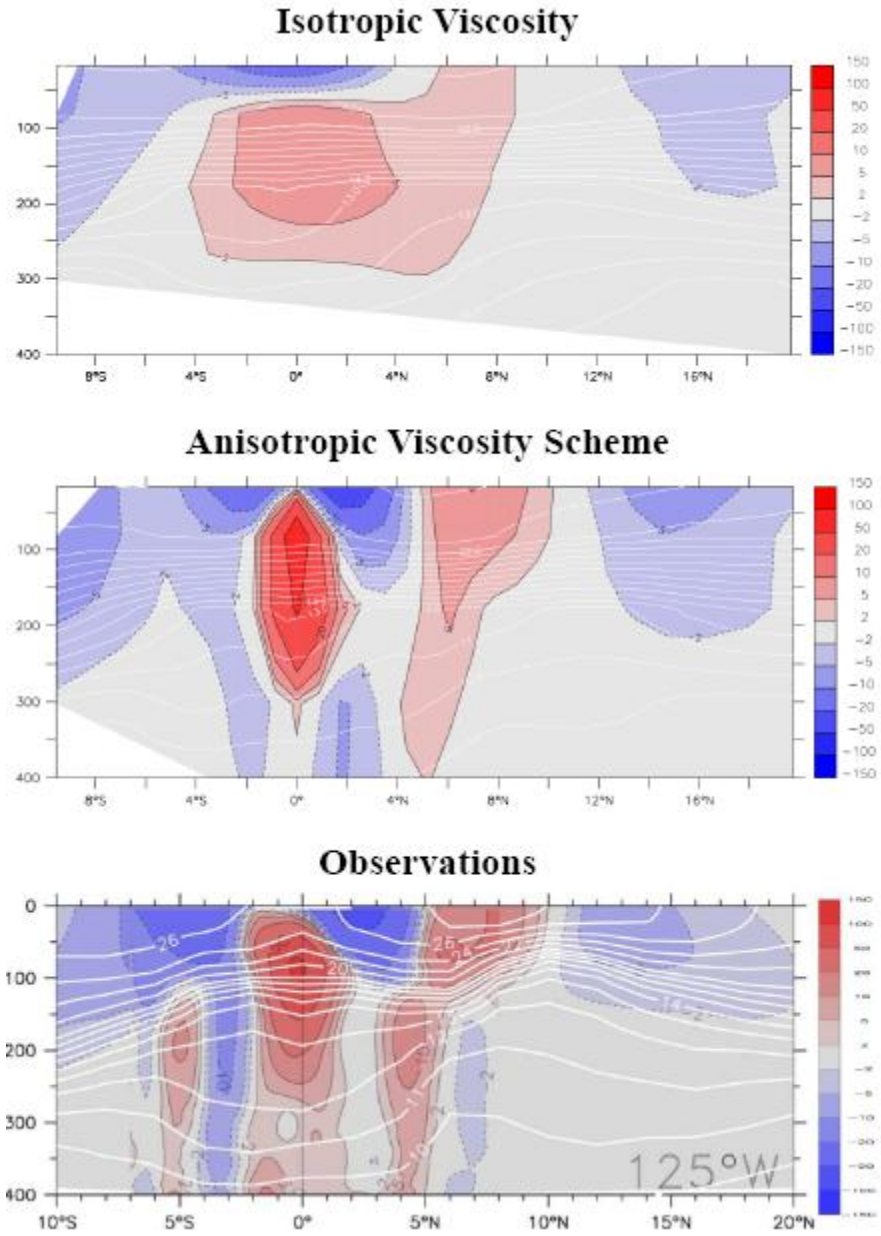


Figure S1-2. Annual averaged zonal velocity (cm s^{-1}) along 125°W using (a) an isotropic viscosity, (b) the anisotropic viscosity scheme and (c) observations from *Kessler* [2006].

Supplementary Material 2: Marine Ecosystem Model

This appendix provides a description of the parameters used in the full set of time-dependent equations in the marine ecosystem model. It suffices to note that the equations for total nitrogen ($^{14}\text{N} + ^{15}\text{N}$) ecosystem variables are identical to the ones of ^{15}N if $R_X = \beta_X/(1+\beta_X) = 1$, which are located in Appendix A.

The function J_O provides the growth rate of non-diazotrophic phytoplankton, determined from irradiance (I), NO_3^- and PO_4^{3-} ,

$$J_O(I, \text{NO}_3^-, \text{PO}_4^{3-}) = \min(J_{OI}, J_{Omax}u_N, J_{Omax}u_P) \quad (\text{S2-1})$$

The maximum growth rate is dependent only on temperature (T):

$$J_{Omax} = a \cdot \exp(T/T_b) \quad (\text{S2-2})$$

such that growth rates increase by a factor of ten over the temperature range of -2 to 34 °C. We use $a=0.11 \text{ d}^{-1}$ for the maximum growth rate at 0 °C which was determined to optimize surface nutrient concentrations. Under nutrient-replete conditions, the light-limited growth rate J_{OI} is calculated according to:

$$J_{OI} = \frac{J_{Omax} \alpha I}{[J_{Omax}^2 + (\alpha I)^2]^{1/2}} \quad (S2-3)$$

where α is the initial slope of the photosynthesis vs. irradiance (P-I) curve. The calculation of the photosynthetically active shortwave radiation I and the method of averaging equation (S2-3) over one day is outlined in *Schmittner et al.* [2005]. This version also includes in the correction for the error in the calculation of light limitation in previous versions [*Schmittner et al.*, 2008b]. Nutrient limitation is represented by the product of J_{Omax} and the nutrient uptake rates, $u_N = \text{NO}_3^- / (k_N + \text{NO}_3^-)$ and $u_P = \text{PO}_4^{3-} / (k_P + \text{PO}_4^{3-})$, with $k_P = k_N R_{P:N}$ providing the respective nutrient uptake rates.

Diazotrophs grow according to the same principles as the general phytoplankton class, but are disadvantaged in nitrate-bearing waters by a lower maximum growth rate, J_{Dmax} , which is set to zero below 15°C:

$$J_{Dmax} = c_D \max[0, a(\exp(T / T_b) - 2.61)] \quad (S2-4)$$

The coefficient c_D handicaps diazotrophs by dampening the increase of their maximal growth rate versus that of the general phytoplankton class with rising temperature. We use $c_D = 0.5$, such

that the increase per °C warming of diazotrophs is 50% that of other phytoplankton. This handicap is further decreased to $c_D = 0.25$ when aeolian dissolved Fe deposition is below $10 \mu\text{mol Fe m}^2 \text{ yr}^{-1}$ [Fan *et al.*, 2006] and smoothly transitions to $c_D = 0.5$ outside of these areas. However, diazotrophs have an advantage in that their growth rate is not limited by NO_3^- concentrations:

$$J_D(I, PO_4) = \min(J_{DI}, J_{Dmax}u_P) \quad (\text{S2-5})$$

although they do take up NO_3^- if it is available (see term 5 in the right hand side of eq. C10). The N:P of model diazotrophs is equal to the general phytoplankton class (16:1). Although there is evidence that the best-studied diazotrophs of the genus *Trichodesmium* have much higher N:P [e.g. Sanudo-Wilhelmy *et al.*, 2004], the more abundant unicellular diazotrophs are uncharacterized [Karl *et al.*, 2002] and for simplicity of interpretation we opted to keep the N:P of both phytoplankton groups identical.

The first order mortality rate of phytoplankton is linearly dependent on their concentration, P_O . DOM and the microbial loop are folded into a single fast-remineralization process, which is the product of P_O and the temperature dependent term

$$\mu_P = \mu_{PO} \exp(T / T_b). \quad (\text{S2-6})$$

83

84 Diazotrophs die at a linear rate where half of the resulting detritus is included into the fast-
85 remineralization process.

86

87 Grazing of phytoplankton by zooplankton is unchanged from *Schmittner et al.* [2005]. Detritus is
88 generated from sloppy zooplankton feeding and mortality among the three classes of plankton,
89 and is the only component of the ecosystem model to sink. It does so at a speed of

90

$$91 \quad w_D = \begin{cases} w_{D0} + m_w z, z \leq 1000m \\ w_{D0} + m_w 1000m, z > 1000m \end{cases}, \quad (S2-7)$$

92

93 increasing linearly with depth z from $w_{D0}=7 \text{ md}^{-1}$ at the surface to 40 md^{-1} at 1 km depth and
94 constant below that, consistent with observations [*Berelson, 2002*]. The remineralization rate of
95 detritus is temperature dependent and decreases by a factor of 5 in suboxic waters, as O_2
96 decreases from $5 \text{ }\mu\text{M}$ to $0 \text{ }\mu\text{M}$:

97

$$98 \quad \mu_D = \mu_{D0} \exp(T/T_b)[0.65+0.35\tanh(O_2 - 6)] \quad (S2-8)$$

99

100 Remineralization transforms the N and P content of detritus to NO_3^- and PO_4^{3-} . Photosynthesis
 101 produces oxygen, while respiration consumes oxygen, at rates equal to the consumption and
 102 remineralization rates of PO_4 , respectively, multiplied by the constant ratio $R_{O:P}$. Dissolved
 103 oxygen exchanges with the atmosphere in the surface layer (F_{sfc}) according to the OCMIP
 104 protocol.

105

106 Oxygen consumption in suboxic waters ($\text{O}_2 < \sim 5 \mu\text{M}$) is inhibited, according to

107

$$108 \quad r_{sox}^{O_2} = 0.5 \left[\tanh(O_2 - 5) + 1 \right] \quad (\text{S2-9})$$

109

110 but is replaced by the oxygen-equivalent oxidation of nitrate,

111

$$112 \quad r_{sox}^{NO_3} = 0.5 \left[1 - \tanh(O_2 - 5) \right]. \quad (\text{S2-10})$$

113

114 Denitrification consumes nitrate at a rate of 80% of the oxygen equivalent rate, as NO_3 is a more
 115 efficient oxidant on a mol per mol basis (i.e. one mol of NO_3 can accept $5e^-$ while 1 mol of O_2
 116 can accept only $4e^-$). Note that the model does not include sedimentary denitrification, which
 117 would provide a large and less time-variant sink for fixed nitrogen.

118

119 We implement the sedimentary denitrification metamodel equation of *Middleburg et al.* [1996]
120 which parameterizes sedimentary denitrification based on the labile carbon flux (F_c) into the
121 sediments:

122

$$123 \quad SedDeni = \alpha_{SD} \cdot 10^{\wedge} \left[-0.9543 + 0.7662 \cdot \log(F_c) - 0.2350 \cdot \log(F_c)^2 \right] \quad (S2-11)$$

124

125 SedDeni is the amount of NO_3^- that is removed from the bottom water. We assume that the flux
126 of labile carbon (F_c) occurs at a ratio of $R_{C:N} = 6.6$ of the sinking nitrogen in the organic detritus.
127 Because the continental shelves are not well resolved in the model, we use an additional
128 parameterization for them. The portion of each ocean grid box that is covered by a shallower
129 continental shelf is recorded as the SHELF coefficient. The labile organic carbon (F_c) that is
130 included in the sedimentary denitrification model in the shelf parameterization is the amount of
131 organic carbon that sinks into the portion of the grid box covered by a shallower continental shelf
132 (i.e., $\text{SHELF} \times F_c$). In the model, ~80% of the sedimentary denitrification occurs within this
133 shelf parameterization. The remaining organic matter (i.e., $F_c \times [1 - \text{SHELF}]$) continues to sink
134 to greater depths. The physical circulation model's inability to fully resolve coastal upwelling
135 systems also underestimates primary production and sinking carbon fluxes on the continental
136 shelves and hence sedimentary denitrification. To account for this, we arbitrarily multiply the
137 sedimentary denitrification rate by a coefficient α_{SD} tuned to 6.5 to set the global deep oceanic
138 $\delta^{15}\text{NO}_3$ average in the model to ~5‰. Without this parameterization, the deep oceanic $\delta^{15}\text{NO}_3$

139 average slowly drifts well above 10‰. The tuning parameter α_{SD} was also tested at the values of
140 6 and 7, which resulted in deep oceanic $\delta^{15}\text{NO}_3$ averages of 5.2‰ and 4.95‰, respectively.
141 Figure 2 shows the spatial distribution of sedimentary denitrification.

<i>Parameter</i>	<i>Symbol</i>	<i>Value</i>	<i>Units</i>
<i>Phytoplankton (P_O, P_D) Coefficients</i>			
Initial slope of P-I curve	α	0.1	$(\text{W m}^{-2})^{-1} \text{d}^{-1}$
Photosynthetically active radiation	PAR	0.43	
Light attenuation in water	k_w	0.04	m^{-1}
Light attenuation through phytoplankton	k_c	0.03	$\text{m}^{-1}(\text{mmol m}^{-3})^{-1}$
Light attenuation through sea ice	k_i	5	m^{-1}
Maximum growth rate	a	0.2	d^{-1}
Half-saturation constant for N uptake	k_N	0.7	mmol m^{-3}
Specific mortality rate	μ_P	0.05	d^{-1}
Fast recycling term (microbial loop)	μ_{P0}^*	0.04	d^{-1}
Diazotrophs' handicap	c_D	0.5	
<i>Zooplankton (Z) Coefficients</i>			
Assimilation efficiency	γ_I	0.925	
Maximum grazing rate	g	1.575	d^{-1}
Prey capture rate	ε	1.6	$(\text{mmol m}^{-3})^{-2} \text{d}^{-1}$
Mortality	μ_Z	0.34	$(\text{mmol m}^{-3})^{-2} \text{d}^{-1}$

<i>Parameter</i>	<i>Symbol</i>	<i>Value</i>	<i>Units</i>
Excretion	γ_2	0.05	d ⁻¹
<i>Detritus (D) Coefficients</i>			
Remineralization rate	μ_{D0}	0.048	d ⁻¹
Sinking speed at surface	w_{D0}	7	m d ⁻¹
Increase of sinking speed with depth	m_w	0.04	d ⁻¹
E-folding temperature of biological rates	T_b	15.65	°C
<i>Other Coefficients</i>			
Molar elemental ratios	$R_{O:N}$	10.6	
	$R_{N:P}$	16	

143 **Table S2-1:** Marine Ecosystem Parameters.

144

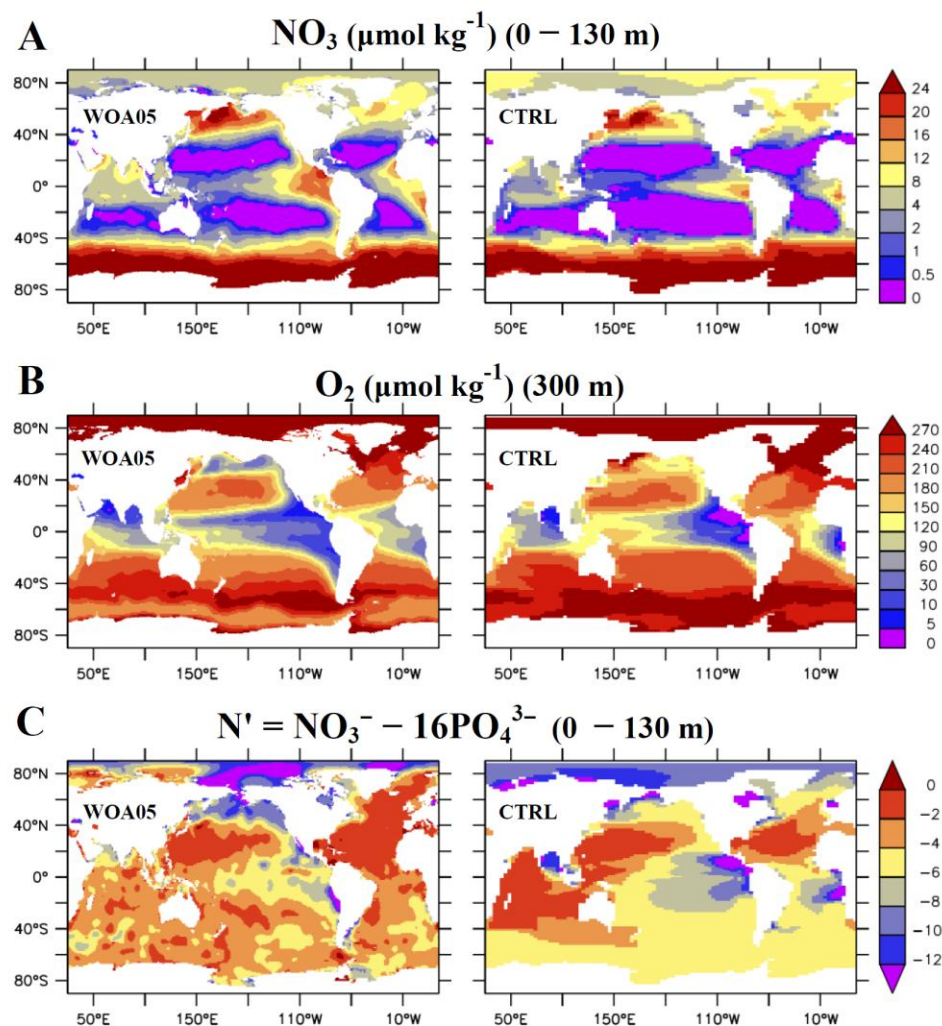


Figure S2-2. Top Panel: Comparison between annual WOA05 observations [Garcia *et al.*, 2006] with CTRL of (A) surface NO_3 , (B) subsurface O_2 , and (C) surface N' .